



# Time-frequency decomposition of multivariate multicomponent signals



Ljubiša Stanković<sup>a,\*</sup>, Danilo Mandić<sup>b</sup>, Miloš Daković<sup>a</sup>, Miloš Brajović<sup>a</sup>

<sup>a</sup>Electrical Engineering Department, University of Montenegro, Montenegro

<sup>b</sup>Imperial College London, United Kingdom

## ARTICLE INFO

### Article history:

Received 27 April 2017

Revised 19 July 2017

Accepted 1 August 2017

Available online 8 August 2017

### Keywords:

Multivariate signals

Time-frequency signal analysis

Analytic signal

Instantaneous frequency

Signal decomposition

Concentration measure

Estimation

## ABSTRACT

A solution of the notoriously difficult problem of characterization and decomposition of multicomponent multivariate signals which partially overlap in the joint time-frequency domain is presented. This is achieved based on the eigenvectors of the signal autocorrelation matrix. The analysis shows that the multivariate signal components can be obtained as linear combinations of the eigenvectors that minimize the concentration measure in the time-frequency domain. A gradient-based iterative algorithm is used in the minimization process and for rigor, a particular emphasis is given to dealing with local minima associated with the gradient descent approach. Simulation results over illustrative case studies validate the proposed algorithm in the decomposition of multicomponent multivariate signals which overlap in the time-frequency domain.

Crown Copyright © 2017 Published by Elsevier B.V. All rights reserved.

## 1. Introduction

Signals with time-varying spectral content are not readily characterized by the conventional Fourier analysis, and are commonly studied within the time-frequency (TF) analysis [1–8]. Research in this field has resulted in numerous representations and algorithms which have been almost invariably introduced for the processing of univariate signals, with most frequent characterization through amplitude and frequency-modulated oscillations [6,9].

Recently, the progress in sensing technology for multidimensional signals has been followed by a growing interest in time-frequency analysis of such multichannel (multivariate and/or multidimensional) data. Namely, developments in sensor technology have made accessible multivariate data. Indeed, the newly introduced concept of modulated bivariate and trivariate data oscillations (3D inertial body sensor, 3D anemometers [9]) and the generalization of this concept to an arbitrary number of channels have opened the way to exploit multichannel signal interdependence in the joint time-frequency analysis [10–12].

The concept of multivariate modulated oscillations has been proposed in [10], under the restricting assumption that one common oscillation fits best all individual channel oscillations. In other words, a joint instantaneous frequency (IF) aims to characterize multichannel data by capturing the combined frequency of all individual channels. It is defined as a weighted average of the IFs

in all individual channels. The deviation of multivariate oscillations in each channel from the joint IF is characterized by the joint instantaneous bandwidth. With the aim to estimate the joint IF of multichannel signals, the synchrosqueezed transform, a highly concentrated time-frequency representation (TFR) belonging to the class of reassigned TF techniques, has been recently extended to the multivariate model [9]. Following the same aim of extracting the local oscillatory dynamics of a multivariate signal, the wavelet ridge algorithm has also been introduced within the multivariate framework [10]. Another very popular concept, empirical mode decomposition (EMD), has been studied for multivariate data, [18–22]. However, successful EMD-based multicomponent signal decomposition is possible only for signals which exhibit nonoverlapping components in the TF plane.

By virtue of high concentration and many other desirable properties, the Wigner distribution is commonly exploited in numerous IF estimators developed within the TF signal analysis [6–8]. However, in the case of multicomponent signals, undesirable oscillatory interferences known as cross-terms appear, sometimes masking the presence of desirable auto-terms. To this end, other representations have been developed, commonly aiming to preserve Wigner distribution concentration, while suppressing the cross-terms. One such algorithm is the S-method [6] which was also used as a basis for the multi-component signal decomposition algorithm, proposed in [1]. This particular type of decomposition makes it possible to analyze and characterize signal components independently, allowing the IF estimation for each separate component [1–4].

\* Corresponding author.

E-mail addresses: [l.stankovic@ieee.org](mailto:l.stankovic@ieee.org), [ljubisa@ac.me](mailto:ljubisa@ac.me) (L. Stanković).

In this paper, multivariate Wigner distribution is studied as the basis of multicomponent multichannel signal decomposition. Namely, the strong interdependence of modulations of individual components within all the available data channels is exploited in the joint TF analysis, leading to a reduction of undesirable oscillations present in cross-terms. The inverse multivariate Wigner distribution matrix is decomposed into eigenvectors which contain signal components in the form of their linear combination. Further, a steepest-descent algorithm that enables a fast search for a linear combination of eigenvectors that produces the best possible components concentration is applied. Using the advantages of multichannel interdependence, the proposed TF-based decomposition is shown to be successful in the case of multivariate signals which overlap in the TF plane, while preserving the integrity of each extracted signal component.

Notice that the conventional time-frequency decomposition techniques cannot separate crossing components of arbitrary forms, which may appear in various signal processing applications. One such scenario is in radar signal processing, where reflecting points may assume the same velocity along the line-of-sight. These components will cross in the time-frequency (time-Doppler) representation. The same effect appears when the target signature crosses with the clutter or stationary body reflecting component in the time-frequency representation of radar signal return. The proposed method assumes that multiple phase independent received signals are available. They can be obtained using polarization or multiple antenna systems [23]. Signals with low frequency variations, when the amplitude changes are of the same order as the phase changes, can also be treated as signals with crossing components. Such are the ECG signals, for example. Multivariate forms of these signals are obtained using multiple sensors at different locations. The presented approach can be applied to the decomposition of this class of signals as well.

The paper is organized as follows. Basic theory regarding multivariate TF signal analysis is presented in Section 2. In Section 3, the Wigner distribution of multivariate multicomponent signals is analyzed. In Section 4, we present the basic theory leading to the decomposition of multivariate multi-component signals, whereas the decomposition algorithm is presented in Section 5. The theory is verified through several numerical examples in Section 6.

## 2. Multivariate time-frequency analysis

Consider a multivariate signal

$$\mathbf{x}(t) = \begin{bmatrix} a_1(t)e^{j\phi_1(t)} \\ a_2(t)e^{j\phi_2(t)} \\ \vdots \\ a_N(t)e^{j\phi_N(t)} \end{bmatrix} \quad (1)$$

obtained by measuring a complex-valued signal  $x(t)$  with  $N$  sensors, where by each sensor the amplitude and phase of the original signal are modified to give  $a_i(t)\exp(j\phi_i(t)) = \alpha_i x(t)\exp(j\varphi_i)$ . If the measured signal is real-valued, its analytic extension

$$x(t) = x_R(t) + jH\{x_R(t)\}$$

is commonly used, with  $x_R(t)$  being real-valued measured signal and  $H\{x_R(t)\}$  its Hilbert transform. Analytic signal contains only nonnegative frequencies and the real-valued counterpart can be reconstructed. This form of signal is especially important in the instantaneous frequency interpretation within the time-frequency moments framework.

Since all time-frequency representations may be considered as smoothed versions of the Wigner distribution, this distribution will be the starting point for a review of time-frequency based multivariate signal analysis. The Wigner distribution of a multivariate

signal  $\mathbf{x}(t)$  is defined as

$$WD(\omega, t) = \int_{-\infty}^{\infty} \mathbf{x}^H(t - \frac{\tau}{2})\mathbf{x}(t + \frac{\tau}{2})e^{-j\omega\tau} d\tau, \quad (2)$$

where  $\mathbf{x}^H(t)$  is a Hermitian transpose of the vector  $\mathbf{x}(t)$ .

The inverse Wigner distribution is then given by

$$\mathbf{x}^H(t - \frac{\tau}{2})\mathbf{x}(t + \frac{\tau}{2}) = \frac{1}{2\pi} \int_{-\infty}^{\infty} WD(\omega, t)e^{j\omega\tau} d\omega. \quad (3)$$

The center of mass in the frequency axis of the Wigner distribution of a multivariate signal  $\mathbf{x}(t)$ , defined by (1), is given by

$$\langle \omega(t) \rangle = \frac{\int_{-\infty}^{\infty} \omega WD(\omega, t) d\omega}{\int_{-\infty}^{\infty} WD(\omega, t) d\omega}$$

or, more explicitly

$$\begin{aligned} \langle \omega(t) \rangle &= \frac{\frac{d}{d\tau} [\mathbf{x}^H(t - \frac{\tau}{2})\mathbf{x}(t + \frac{\tau}{2})]_{\tau=0}}{\mathbf{x}^H(t - \frac{\tau}{2})\mathbf{x}(t + \frac{\tau}{2})_{\tau=0}} \\ &= \frac{1}{2j} \frac{[\mathbf{x}^H(t)\mathbf{x}'(t) - \mathbf{x}'^H(t)\mathbf{x}(t)]}{\mathbf{x}^H(t)\mathbf{x}(t)}, \end{aligned}$$

where  $\mathbf{x}'(t) = d\mathbf{x}(t)/dt$  denotes derivative in time.

The expression for instantaneous frequency of a multivariate signal follows straightforwardly from the previous relation in the form:

$$\langle \omega(t) \rangle = \frac{\sum_{n=1}^N \phi'_n(t) a_n^2(t)}{\sum_{n=1}^N a_n^2(t)}. \quad (4)$$

If a multivariate signal is obtained by sensing a monocomponent signal  $x(t)$  as  $a_i(t)\exp(j\phi_i(t)) = \alpha_i x(t)\exp(j\varphi_i)$  with  $x(t) = A(t)\exp(j\psi(t))$  and  $|dA(t)/dt| \ll |d\psi(t)/dt|$ , then  $\langle \omega(t) \rangle = d\psi(t)/dt$ , since  $d\phi_i(t)/dt = d\psi(t)/dt$ . The condition for amplitude and phase variations of real-valued monocomponent signals  $a_i(t)\cos(\phi_i(t))$  can be defined by Bedrosian's product theorem [13]. It states that the complex analytic signal  $a_i(t)\exp(j\phi_i(t)) = a_i(t)\cos(\phi_i(t)) + jH\{a_i(t)\cos(\phi_i(t))\}$  is a valid representation of the real amplitude-phase signal  $a_i(t)\cos(\phi_i(t))$  if the spectrum of  $a_i(t)$  is nonzero only within the frequency range  $|\omega| < B$  and the spectrum of  $\cos(\phi_i(t))$  occupies nonoverlapping higher frequency range. A signal is monocomponent if the spectrum of  $a_i(t)$  is of lowpass type.

This analysis can be generalized to other time-frequency and time-scale signal representations.

A deviation of the signal spectral content from the instantaneous frequency is described by the local second order moments (instantaneous bandwidths). The expression for the instantaneous bandwidth is obtained from

$$\begin{aligned} \sigma_\omega^2(t) &= \frac{1}{2\pi \mathbf{x}^H(t)\mathbf{x}(t)} \int_{-\infty}^{\infty} \omega^2 WD(t, \omega) d\omega - \langle \omega(t) \rangle^2 \\ &= \frac{-\frac{d^2}{d\tau^2} [\mathbf{x}^H(t - \frac{\tau}{2})\mathbf{x}(t + \frac{\tau}{2})]_{\tau=0}}{\mathbf{x}^H(t)\mathbf{x}(t)} - \langle \omega(t) \rangle^2. \end{aligned}$$

For the signal in (1) it has the following form:

$$\sigma_\omega^2(t) = \frac{\sum_{n=1}^N (a'_n(t))^2 - \sum_{n=1}^N a_n(t)a''_n(t)}{2 \sum_{n=1}^N a_n^2(t)}.$$

In general, for the case of multicomponent signals, the components are localized over more than one instantaneous frequency.

## 3. Multicomponent signals

Consider a multicomponent signal

$$x(t) = \sum_{p=1}^P x_p(t)$$

the components of which are of the form

$$x_p(t) = A_p(t)e^{j\psi_p(t)}$$

with the component amplitudes  $A_p(t)$  having a slow-varying dynamics as compared to the variations of the phases  $\psi_p(t)$ , i.e.,  $|dA_p(t)/dt| \ll |d\psi_p(t)/dt|$ . The corresponding multivariate signal is then given by

$$\mathbf{x}(t) = \sum_{p=1}^P \begin{bmatrix} \alpha_{p1}x_p(t)e^{j\varphi_{p1}} \\ \alpha_{p2}x_p(t)e^{j\varphi_{p2}} \\ \vdots \\ \alpha_{pN}x_p(t)e^{j\varphi_{pN}} \end{bmatrix}. \quad (5)$$

The individual components  $x_1(t), \dots, x_p(t)$ , measured at different sensors, differ in their amplitudes and phases but share the instantaneous frequency  $\omega_p(t) = d\psi_p(t)/dt$  corresponding to  $\langle \omega_p(t) \rangle$  in (4), with  $p$  being the component index.

The Wigner distribution of this multivariate multicomponent signal is

$$WD(\omega, t) = \sum_{p=1}^P \sum_{q=1}^P \sum_{i=1}^N \int_{-\infty}^{\infty} \alpha_{pi}\alpha_{qi}x_p(t + \frac{\tau}{2})x_q^*(t - \frac{\tau}{2})e^{j(\varphi_{pi}-\varphi_{qi})}e^{-j\omega\tau}d\tau,$$

with  $i$  being the sensor index. It may be written as a sum of auto-terms and cross-terms

$$\begin{aligned} WD(\omega, t) &= \sum_{p=1}^P \sum_{i=1}^N \alpha_{pi}^2 \int_{-\infty}^{\infty} x_p(t + \frac{\tau}{2})x_p^*(t - \frac{\tau}{2})e^{-j\omega\tau}d\tau \\ &+ \sum_{p=1}^P \sum_{q=1}^P \sum_{\substack{i=1 \\ q \neq p}}^N \alpha_{pi}\alpha_{qi} \int_{-\infty}^{\infty} x_p(t + \frac{\tau}{2})x_q^*(t - \frac{\tau}{2})e^{j(\varphi_{pi}-\varphi_{qi})}e^{-j\omega\tau}d\tau. \\ &= WD_a(\omega, t) + WD_c(\omega, t) \end{aligned} \quad (6)$$

The phase shifts of the components of the multivariate signal in (6) cancel out in the auto-terms  $WD_a(\omega, t)$ . This important property implies that the auto-terms, obtained from each variate of a multivariate signal, are summed in-phase, independently from the (different) initial phases in the individual signal components. In the cross-terms, the phase shifts do not cancel-out in the resulting  $WD_c(\omega, t)$ , leading to an out-of-phase summation. The cross-terms in the multivariate case are a sum of  $N$  signals with arbitrary (random) phases. They are consequently reduced with respect to the Wigner distribution of an univariate signal. Therefore, for a large  $N$  we would expect the auto-terms only, while the cross-terms will tend to a small value with respect to the auto-terms. It is expected that the cross-terms, for a large number of sensors  $N$ , behave as a time-frequency dependent zero-mean Gaussian random variable, the variance of which depends on the cross-terms value,  $\text{var}\{WD(\omega, t)\} = \sigma^2(WD_c(\omega, t))$ . The auto-terms are deterministic for a given signal, since they do not depend on random phases, as seen in the corresponding Wigner distribution term  $WD_a(\omega, t)$ . This means that for a large  $N$

$$WD(\omega, t) \sim \mathcal{N}(WD_a(\omega, t), \sigma^2(WD_c(\omega, t))).$$

#### 4. Inversion and signal decomposition

The inversion of a Wigner distribution of a multivariate signal in the analog domain is given by

$$\mathbf{x}^H(t_2)\mathbf{x}(t_1) = \frac{1}{2\pi} \int_{-\infty}^{\infty} WD\left(\frac{t_1+t_2}{2}, \omega\right)e^{j\omega(t_1-t_2)}d\omega.$$

By the discretization of angular frequency,  $\omega = k\Delta\omega$ , and the time,  $t_1 = n_1\Delta t$ ,  $t_2 = n_2\Delta t$ , with an appropriate definition of discrete values, we easily obtain

$$\mathbf{x}^H(n_2)\mathbf{x}(n_1) = \frac{1}{K+1} \sum_{k=-K/2}^{K/2} WD\left(\frac{n_1+n_2}{2}, k\right)e^{j\frac{\pi}{K+1}k(n_1-n_2)}. \quad (7)$$

Upon introducing the notation

$$R(n_1, n_2) = \frac{1}{K+1} \sum_{k=-K/2}^{K/2} WD\left(\frac{n_1+n_2}{2}, k\right)e^{j\frac{\pi}{K+1}k(n_1-n_2)}, \quad (8)$$

we obtain

$$R(n_1, n_2) = \mathbf{x}^H(n_2)\mathbf{x}(n_1). \quad (9)$$

Therefore, for multicomponent multivariate signals, the inversion produces a matrix with the elements of the form

$$R(n_1, n_2) = \sum_{i=1}^N \sum_{p=1}^P \sum_{q=1}^P \alpha_{pi}\alpha_{qi}x_p(n_1)x_q^*(n_2)e^{j(\varphi_{pi}-\varphi_{qi})}. \quad (10)$$

If we now use the assumption that the cross-terms in the Wigner distribution of multivariate signals can be neglected with respect to the auto-terms summed in phase, this yields

$$R(n_1, n_2) = \sum_{i=1}^N \sum_{p=1}^P a_{pi}^2 x_p(n_1)x_p^*(n_2) = \sum_{p=1}^P B_p x_p(n_1)x_p^*(n_2) \quad (11)$$

where  $B_p = \sum_{i=1}^N \alpha_{pi}^2$ .

As for any square matrix, the eigenvalue decomposition of a  $K \times K$  dimensional matrix  $\mathbf{R}$  gives

$$\mathbf{R} = \mathbf{Q}\mathbf{\Lambda}\mathbf{Q}^T = \sum_{p=1}^K \lambda_p \mathbf{q}_p(n)\mathbf{q}_p^*(n), \quad (12)$$

where  $\lambda_p$  are the eigenvalues and  $\mathbf{q}_p(n)$  are the corresponding eigenvectors of  $\mathbf{R}$ . Note that the eigenvectors  $\mathbf{q}_p(n)$  are orthonormal.

For a  $P$ -component signal, in a noiseless case, the elements of this matrix are

$$R(n_1, n_2) = \sum_{p=1}^P \lambda_p q_p(n_1)q_p^*(n_2). \quad (13)$$

Let us consider several special cases:

- 1) For a univariate signal and the Wigner distribution, the signal itself is equal to the eigenvector  $\mathbf{q}_1(n)$ , up to a scaling by a complex-valued constant [1], with the corresponding eigenvalues  $\lambda_1 = E_x$ ,  $\lambda_2 = 0, \dots, \lambda_K = 0$ . The fact that the Wigner distribution based inversion produces only one nonzero eigenvalue is also used to check if a given two-dimensional function is a valid Wigner distribution.
- 2) If the components of a multicomponent univariate signal do not overlap in the time-frequency plane, then it is possible to calculate the distribution which will be equal to a sum of the Wigner distributions of the individual signal components. This calculation is performed using the S-method and the property [1]:

$$SM(n, k) = \sum_{p=1}^P WD_p(n, k). \quad (14)$$

Since the non-overlapping components are orthogonal, the eigenvalue decomposition will produce

$$B_p \mathbf{x}_p(n) = \lambda_p \mathbf{q}_p(n), \quad p = 1, 2, \dots, P.$$

where  $B_p$  is a constant. Note that, by definition, the energy of the corresponding eigenvector is equal to 1,

$$\|\mathbf{q}_p(n)\|^2 = 1. \quad (15)$$

We can conclude that

$$B_p \mathbf{x}_p(n)\mathbf{x}_p^*(n) = \left(\sqrt{\lambda_p} \mathbf{q}_p(n)\right) \left(\sqrt{\lambda_p} \mathbf{q}_p(n)\right)^*$$

and

$$\lambda_p = \left\| \sqrt{\lambda_p} \mathbf{q}_p(n) \right\|^2 = \left\| B_p \mathbf{x}_p(n) \right\|^2 = \sum_{n=-K/2}^{K/2} B_p x_p^2(n) = B_p E_{x_p},$$

where  $E_{x_p}$  is the energy of the signal  $p$ th component. The eigenvector  $\mathbf{q}_p(n)$  is equal to the signal vector  $\mathbf{x}_p(n)$ , up to the constant amplitude and phase ambiguity.

- 3) If the signal components  $\mathbf{x}_p(n)$  overlap in the frequency plane, then the decomposition on the individual components is not possible using the state-of-art methods, except in cases of quite specific signal forms (such as linear frequency modulated signals, using chirplet transform, Radon transform or similar techniques [14,15], or for sinusoidally modulated signals using inverse Radon transform, [16,17]). In general, these kinds of signals cannot be separated into individual components in the univariate case. However, the multivariate form of signals reduces (changes) the cross-terms in the Wigner distribution, thus offering a possibility to decompose the components which overlap in the time-frequency plane.

## 5. Decomposition algorithm

Consider a multicomponent signal of the form (5), with signal components  $\mathbf{x}_p$ ,  $p = 1, 2, \dots, P$  whose supports  $\mathbb{D}_p$  may partially overlap in the time-frequency domain. We also make a realistic assumption that there is no signal component whose time-frequency support completely overlaps with other component, and  $D_1 \leq D_2 \leq \dots \leq D_P$ , where  $D_p$  is the area of the support  $\mathbb{D}_p$ .

The first signal component can be expressed as linear combination of vectors  $\mathbf{q}_p$  with coefficients  $\eta_{1p}$  to give

$$\mathbf{x}_1 = \eta_{11} \mathbf{q}_1 + \eta_{21} \mathbf{q}_2 + \dots + \eta_{P1} \mathbf{q}_P. \quad (16)$$

Since we have assumed that the signal components are well concentrated in the time-frequency domain, we can use a concentration measure in order to find the coefficients  $\eta_{p1}$ . To this end, we form a linear combination of the basis vectors  $\mathbf{q}_p$ , with weighting coefficients  $\beta_p$ ,  $p = 1, 2, \dots, P$ , to arrive at

$$\mathbf{y} = \beta_1 \mathbf{q}_1 + \beta_2 \mathbf{q}_2 + \dots + \beta_P \mathbf{q}_P, \quad (17)$$

and calculate the concentration measure  $\mathcal{M}\{\text{TFR}(n, k)\}$  of the time-frequency representation  $\text{TFR}(n, k)$  of the normalized signal  $\mathbf{y}/\|\mathbf{y}\|_2$ . The choice of the TFR is not crucial here. We can use the spectrogram as the simplest TFR. By solving the concentration measure minimization problem we then obtain the global minimum corresponding to the best concentrated signal component.

The most straightforward way to solve this problem would be to use the zero-norm as the concentration measure of  $\text{TFR}(n, k)$  and perform a direct search over the coefficients  $\beta_p$ ,  $p = 1, 2, \dots, P$ . Then, the coefficients  $\eta_{p1}$  are the solution of the minimization problem

$$[\eta_{11}, \eta_{21}, \dots, \eta_{P1}] = \arg \min_{\beta_1, \dots, \beta_P} \|\text{TFR}(n, k)\|_0.$$

For these values of coefficients  $\|\text{TFR}(n, k)\|_0$  is equal to the area of the best concentrated component support  $D_1$ . If any two the smallest areas are equal we still find one of them.

Note that this minimisation problem has several local minima as the coefficients  $\beta_p$  in  $\mathbf{y} = \beta_1 \mathbf{q}_1 + \beta_2 \mathbf{q}_2 + \dots + \beta_P \mathbf{q}_P$  which correspond to any signal component  $\mathbf{x}_p$  will also produce a local minimum of the concentration measure, equal to the area of corresponding component support. In addition, any linear combination of  $K < P$  signal components  $\mathbf{x}_p$  will also produce a local minimum equal to the area of the union of the supports of included signal components.

After the best concentrated component is detected, the corresponding vector  $\mathbf{q}_1$  is replaced with the extracted signal component. The extracted component is then removed from the remaining vectors  $\mathbf{q}_k$  by subtracting the projection of the extracted component to the vectors  $\mathbf{q}_p$ ,  $p = 2, 3, \dots, P$  (signal deflation procedure [31]). The procedure is repeated with the new set of vectors  $\mathbf{q}_p$  by forming the signal  $\mathbf{y} = \beta_2 \mathbf{q}_2 + \dots + \beta_P \mathbf{q}_P$ , and then by varying the coefficients  $\beta_p$  a new global minimum of the concentration is found, which corresponds to the second signal component. The procedure is iterated  $P$  times.

However, since in practical applications neither the direct search nor the norm-zero concentration can be used, several methods have been developed in literature based on the optimization of problems with several local minima. In general, all these methods can be divided into three large classes: deterministic [27], stochastic [25,26], and heuristic (ant colony optimization [28], genetic algorithm, hill climbing [30], simulated annealing [29], particle swarm optimization...). In this paper we will adapt a gradient-based approach to solve the minimization problem. The zero-norm is replaced by its closest convex counterpart, the one-norm. The proposed algorithm is presented next.

- In the first step, we calculate the matrix  $\mathbf{R}$  of the multivariate signal  $\mathbf{x}(n)$  according to (8) or (9). The number of signal components  $P$  is equal to the number of non-zero eigenvalues of matrix  $\mathbf{R}$ . In the noisy signal cases two approaches for determining the number of components can be utilized: (a) The number of components is assumed. As long as it is larger than or equal to the true number of components  $P$ , the algorithm works properly, producing noise only as the extra components. (b) A threshold is set to separate eigenvalues corresponding to signal components from those corresponding to the noise. This threshold determines the number of components in the decomposition.

- For the time-frequency representation of the signal we can use the spectrogram, the S-method with narrow frequency window (for example  $L_s = 1$ ), or any other appropriate representation. Since these time-frequency representations are quadratic, a concentration measure equivalent to the one-norm should be defined as [24]

$$\mathcal{M}\{\text{TFR}(n, k)\} = \sum_n \sum_k |\text{TFR}(n, k)|^{1/2} \quad (18)$$

where the summation is performed over all available time and frequency indices  $n$  and  $k$ .

The decomposition procedure is outlined in Algorithm 1.

- The measure minimization is implemented by using a steepest descent approach presented in Algorithm 2. Here, we fix the coefficient  $\beta_p = 1$  and vary the real and imaginary parts of the remaining coefficients by  $\pm \Delta$ . The gradient of the normalized measure,  $\gamma_p$ , is then calculated and is used for coefficient update. The initial value of the parameter  $\Delta$  is 0.1 and it is reduced whenever a further coefficients update does not yield a smaller measure.

- When the  $p$ th component is extracted, the corresponding vector  $\mathbf{q}_p$  is replaced with the extracted signal component. The extracted component is then removed from the remaining vectors  $\mathbf{q}_k$  by subtracting the projection of the extracted component to vectors  $\mathbf{q}_k$ ,  $k = p + 1, p + 2, \dots, P$ . In this manner, we ensure that the  $p$ th signal component will not be detected again.

- This procedure is repeated until there is no more updates of vectors  $\mathbf{q}_k$ .

For a two-component signal, the considered minimization problem is now convex, with a single, global, minimum. For a three-component signal, the local minima exists for signals obtained as a sum of any two components. This is the reason why the decomposition procedure is repeated after minimum of the concentration measure is found. In the next iteration, the pair of components corresponding to the local minimum are separated as in the

**Algorithm 1** Multivariate signal decomposition.**Input:**

- Multivariate signal  $\mathbf{x}(n)$

1: Calculate S-Method  $SM(n, k)$  of the multivariate signal  $\mathbf{x}(n)$  and matrix  $\mathbf{R}$  with elements

$$R(n_1, n_2) = \frac{1}{K+1} \sum_{k=-K/2}^{K/2} SM\left(\frac{n_1+n_2}{2}, k\right) e^{j\frac{2\pi}{K+1}k(n_1-n_2)},$$

as in [1]. If the Wigner distribution is used then the  $SM(n, k)$  should be replaced with  $WD(n, k)$ , or we can calculate elements of matrix  $\mathbf{R}$  as  $R(n_1, n_2) = \mathbf{x}^H(n_2)\mathbf{x}(n_1)$ .

2: Find eigenvectors  $\mathbf{q}_i$  and eigenvalues  $\lambda_i$  of matrix  $\mathbf{R}$ .

3:  $P \leftarrow$  number of non-zero eigenvalues

**4: repeat**

5:  $N_{updates} \leftarrow 0$

6: **for**  $i = 1, 2, \dots, P$  **do**

7: Solve minimization problem

$$\min_{\beta_1, \dots, \beta_p} \mathcal{M} \left\{ \text{TFR} \left\{ \frac{1}{C} \sum_{p=1}^P \beta_p \mathbf{q}_p \right\} \right\} \quad \text{subject to } \beta_i = 1$$

where  $\mathcal{M}\{\cdot\}$  is concentration measure,  $\text{TFR}\{\cdot\}$  is time-frequency representation of a provided signal, and

$$C = \sqrt{\sum_{p=1}^P \|\beta_p \mathbf{q}_p\|_2^2}$$

is used to normalize energy of the combined signal to 1. Coefficients  $\beta_1, \beta_2, \dots, \beta_p$  are obtained as a result of the minimization.

8: **if** any  $\beta_p \neq 0, p \neq i$  **then**

$$9: \quad \mathbf{q}_i \leftarrow \frac{1}{C} \sum_{p=1}^P \beta_p \mathbf{q}_p$$

10: **for**  $k = i+1, i+2, \dots, P$  **do**

$$11: \quad s \leftarrow \mathbf{q}_i^H \mathbf{q}_k$$

$$12: \quad \mathbf{q}_k \leftarrow \frac{1}{\sqrt{1-|s|^2}} (\mathbf{q}_k - s\mathbf{q}_i)$$

13: **end for**

$$14: \quad N_{updates} \leftarrow N_{updates} + 1$$

15: **end if**

16: **end for**

17: **until**  $N_{updates} = 0$

**Output:**

- Number of signal components  $P$
- Reconstructed signal components  $\mathbf{q}_1, \mathbf{q}_2, \dots, \mathbf{q}_p$

two-component signal case. For a higher number of signal components, the number of local minima increases. Then several repetitions of the procedure are needed in order to separate the components in an iterative way. Recall that a gradient-based algorithm can find any local minimum, each corresponding to a combinations of  $K < P$  signal components. This means that each local minimum reduces the complexity of decomposition vectors  $\mathbf{q}_p$ , leading to the full signal decomposition in an iterative way. For more details, see [Algorithm 2](#).

**6. Numerical examples**

**Example 1.** Consider a real bivariate signal  $\mathbf{x}(t) = [x_1(t), x_2(t)]^T$ , where the signal from channel  $i$  has the form

**Algorithm 2** Minimization procedure.**Input:**

- Vectors  $\mathbf{q}_1, \mathbf{q}_2, \dots, \mathbf{q}_p$
- Index  $i$  where corresponding vector  $\mathbf{q}_i$  should be kept with unity coefficient  $\beta_i = 1$
- Required precision  $\varepsilon$

$$1: \beta_p = \begin{cases} 1 & \text{for } p = i \\ 0 & \text{for } p \neq i \end{cases}, \quad \text{for } p = 1, 2, \dots, P$$

2:  $M_{old} \leftarrow \infty$

3:  $\Delta = 0.1$

**4: repeat**

$$5: \quad \mathbf{y} \leftarrow \sum_{p=1}^P \beta_p \mathbf{q}_p$$

$$6: \quad M_{new} \leftarrow \mathcal{M} \left\{ \text{TFR} \left\{ \frac{\mathbf{y}}{\|\mathbf{y}\|_2} \right\} \right\}$$

7: **if**  $M_{new} > M_{old}$  **then**

8:  $\Delta \leftarrow \Delta/2$

9:  $\beta_p \leftarrow \beta_p + \gamma_p, \quad \text{for } p = 1, 2, \dots, P$   $\triangleright$  Cancel the last coefficients update

$$10: \quad \mathbf{y} \leftarrow \sum_{p=1}^P \beta_p \mathbf{q}_p$$

11: **else**

12:  $M_{old} \leftarrow M_{new}$

13: **end if**

14: **for**  $p = 1, 2, \dots, P$  **do**

15: **if**  $p \neq i$  **then**

$$16: \quad M_r^+ \leftarrow \mathcal{M} \left\{ \text{TFR} \left\{ \frac{\mathbf{y} + \Delta \mathbf{q}_p}{\|\mathbf{y} + \Delta \mathbf{q}_p\|_2} \right\} \right\}$$

$$17: \quad M_r^- \leftarrow \mathcal{M} \left\{ \text{TFR} \left\{ \frac{\mathbf{y} - \Delta \mathbf{q}_p}{\|\mathbf{y} - \Delta \mathbf{q}_p\|_2} \right\} \right\}$$

$$18: \quad M_i^+ \leftarrow \mathcal{M} \left\{ \text{TFR} \left\{ \frac{\mathbf{y} + j\Delta \mathbf{q}_p}{\|\mathbf{y} + j\Delta \mathbf{q}_p\|_2} \right\} \right\}$$

$$19: \quad M_i^- \leftarrow \mathcal{M} \left\{ \text{TFR} \left\{ \frac{\mathbf{y} - j\Delta \mathbf{q}_p}{\|\mathbf{y} - j\Delta \mathbf{q}_p\|_2} \right\} \right\}$$

$$20: \quad \gamma_p \leftarrow 8\Delta \frac{M_r^+ - M_r^-}{M_{new}} + j8\Delta \frac{M_i^+ - M_i^-}{M_{new}}$$

21: **else**

22:  $\gamma_p \leftarrow 0$

23: **end if**

24: **end for**

25:  $\beta_p \leftarrow \beta_p - \gamma_p, \quad \text{for } p = 1, 2, \dots, P$   $\triangleright$  Coefficients update

26: **until**  $\sum_{p=1}^P |\gamma_p|^2$  is below required precision  $\varepsilon$

**Output:**

- Coefficients  $\beta_1, \beta_2, \dots, \beta_p$

$$\begin{aligned} x_i(t) &= e^{-(t/128)^2} \cos\left((t/16)^4/128 - 8\pi(t/16)^2/64 + \varphi_i\right) \\ &= 0.5e^{-(t/128)^2} \left[ e^{j((t/16)^4/128 - 8\pi(t/16)^2/64 + \varphi_i)} \right. \\ &\quad \left. + e^{-j((t/16)^4/128 - 8\pi(t/16)^2/64 + \varphi_i)} \right] \\ &= x_{1i}(t) + x_{2i}(t), \quad i = 1, 2, \end{aligned} \quad (19)$$

for  $-128 \leq t \leq 128$ , as shown in [Fig. 1](#) (a) (for the first channel). The phases  $\varphi_1 \neq \varphi_2$  are random numbers with a uniform distribution drawn from the interval  $[0, 2\pi]$ . As this signal is real-valued, two symmetric components  $x_{1i}(t)$  and  $x_{2i}(t)$  exist in the Fourier transform and the time-frequency domains. However, these

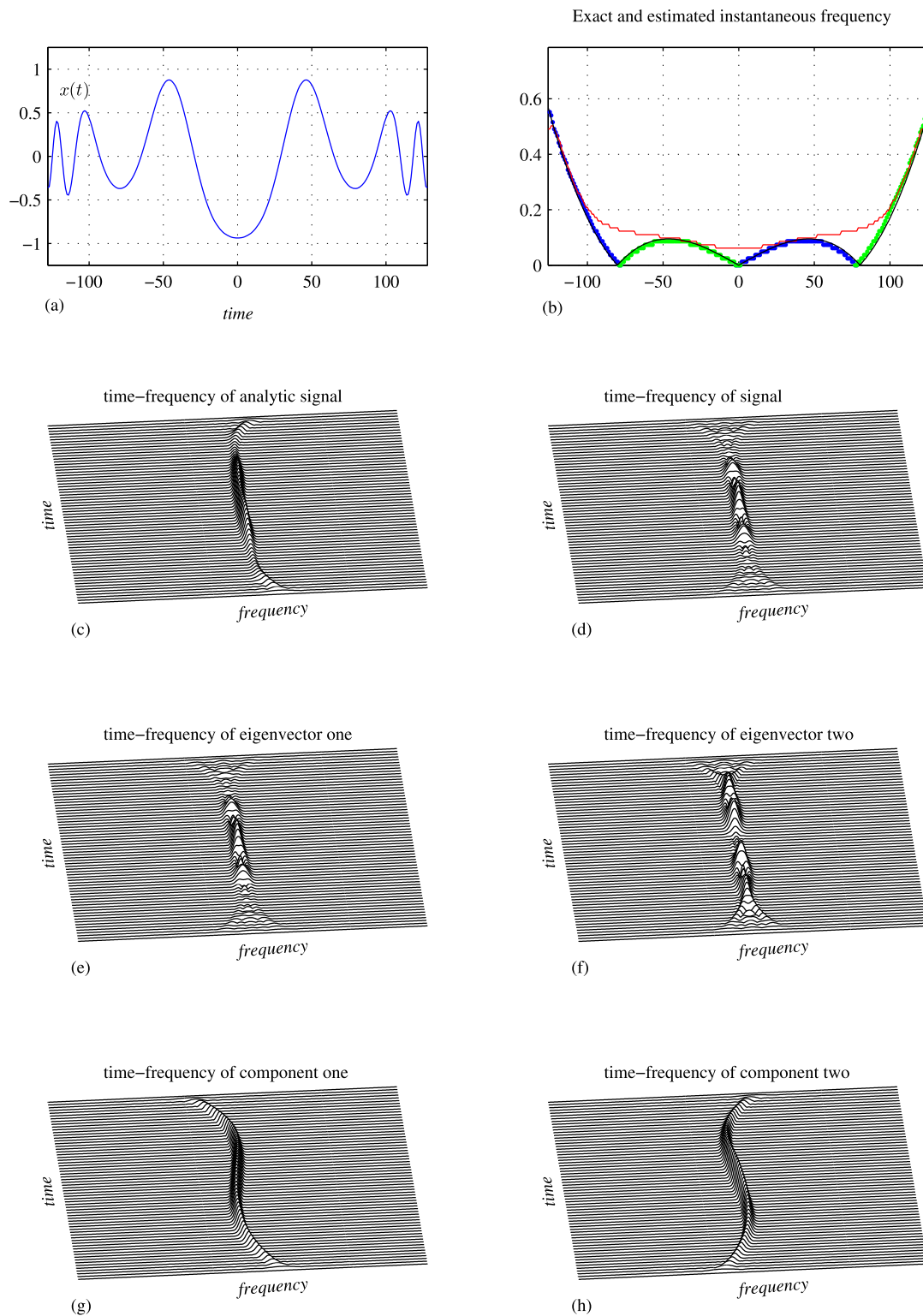


**Fig. 1.** Bivariate real signal analyzed in Example 1. (a) signal shown in time domain. (b) estimation of the IF: black - true IF, red - IF estimation using the analytic signal, green and blue - IF estimation based on components extracted using the proposed approach. (c) PWD of the analytic signal. (d) PWD of the original signal. (e) and (f) PWD of the eigenvectors. (g) and (h) PWD of components extracted using the proposed approach. (For interpretation of the references to colour in this figure legend, the reader is referred to the web version of this article.)

components partially overlap, and thus they are inseparable using these representations.

A common problem is to estimate the instantaneous frequency (IF) of the signal. To this end, for real signals it is usual to calculate its analytic form based on the Hilbert transform. The true IF is

shown in Fig. 1 (b), black line. The time–frequency representation (TFR) of this analytic signal is shown in Fig. 1 (c). However, the IF estimate based on the analytic signal, shown in Fig. 1 (b), red line, obviously significantly differs from the true IF. Namely, the IF estimation based on the standard TFR maxima approach does not appropriately track the IF variations, as they are lost in the

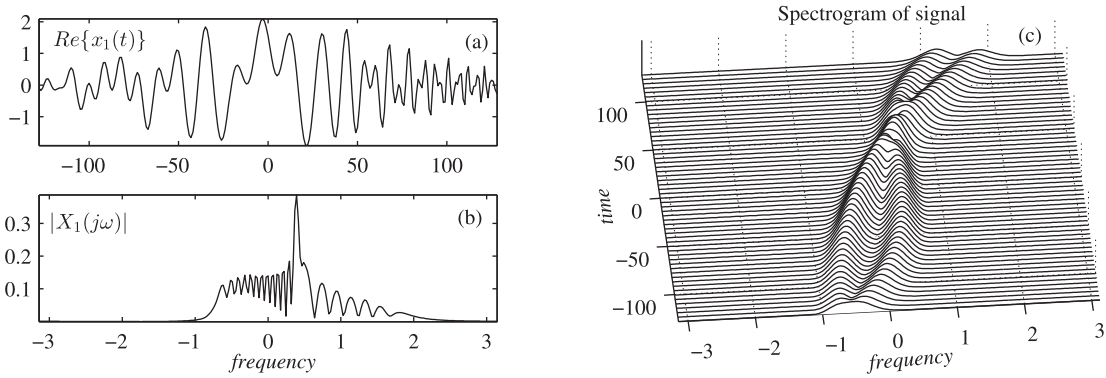


Fig. 2. Bivariate two-component signal shown in: (a) time domain, (b) frequency domain, (c) time-frequency domain (spectrogram).

corresponding TFR due to significant overlapping of the components and the fact that amplitude and phase variations are of the same order. Notice that Bedrosian's product theorem condition for amplitude and phase is not satisfied in this case.

On the other hand, if one calculates the TFR of the original signal (19), the two components  $x_{1i}(t)$  and  $x_{2i}(t)$  overlap in the TF plane, as shown in Fig. 1 (d). These components are also nonlinear and thus, none of the known techniques can be applied for their separation in order to estimate the IF of such overlapping highly nonlinear components. As these components highly overlap, they are not orthogonal, and consequently the S-method based decomposition [1] cannot be applied in a straightforward manner.

However, it is crucial to note that the cross-terms in Wigner distribution (WD) are changed and two eigenvalues different from zero do appear. Therefore, the two corresponding eigenvectors, whose pseudo Wigner distributions (PWD) are shown in Fig. 1 (e) and (f), contain both components, appearing as a linear combination. Using the proposed multi-component decomposition algorithm, we were able to calculate the coefficients  $\beta_1$  and  $\beta_2$ , forming the linear combination (17) of eigenvectors. The minimum concentration (sparsity) measure of this linear combination corresponds to two separate signal components, as shown in Fig. 1 (g) and (h). It can be observed that the IF estimation based on these two TFRs maxima (using positive IF parts), shown in Fig. 1 (b), green and blue dots, is accurate up to the theoretically expected bias caused by the IF non-linearity, which can be further reduced using some well-known IF estimation techniques [6].

**Example 2.** In this example we consider a bivariate two-component signal  $\mathbf{x}(t)$  assuming that each sensor measures

$$x_i(t) = x_{1i}(t) + x_{2i}(t), \quad i = 1, 2 \quad (20)$$

whose components are given by

$$x_{1i}(t) = 1.2e^{-(t/96)^2} e^{-j12\pi(t/16)^2/25+jt^3/256^2+\varphi_{1i}}, \quad (21)$$

$$x_{2i}(t) = 0.9e^{-(t/128)^2} e^{-j\pi t/8+j(t/16)^4/100+\varphi_{2i}}, \quad (22)$$

with phases  $\varphi_{1i}$ ,  $\varphi_{2i}$ ,  $i = 1, 2$  simulated as random numbers with a uniform distribution drawn from the interval  $[0, 2\pi]$ . The real part of the signal from the first channel, and the corresponding Fourier transform are shown in Fig. 2 (a) and (b), whereas the multivariate spectrogram is shown in Fig. 2 (c). It can be observed that the signal components cannot be separated using the spectrogram, without significant auto-term degradation. Note that the two signal components have non-linear frequency modulation, and are thus inseparable using common component decomposition algorithms.

When the proposed algorithm for decomposition of multicomponent signals is applied, aiming to extract each component of the

analyzed signal, then in accordance with the presented theory, the Wigner distribution is used as the initial time-frequency representation for the eigenvalue decomposition. The Wigner distribution of the analyzed signal is shown in Fig. 3 (a) whereas the eigenvalues of autocorrelation matrix  $\mathbf{R}$  are shown in Fig. 3 (b). It can be seen that there are two non-zero eigenvalues containing linear combinations of the signal component. Further steps of the proposed decomposition method assume that a TFR is calculated and the proposed minimization procedure is applied in order to find the coefficients producing the eigenvectors combination (17), leading to the best component concentration. Our numerical experiments have shown that a similar performance of the minimization using Algorithm 2 is obtained when the Wigner distribution, the spectrogram and the S-method are applied as underlying TFRs on the observed eigenvectors. In Fig. 3, we present the results obtained in the case of the Wigner distribution. For visual clarity, pseudo Wigner distribution with Hanning window of length 256 is shown for each eigenvector in Fig. 3 (c) and (e), although the Wigner distribution was used in the minimization procedure. Similar results would be obtained for any other TFR in the minimization step. The pseudo Wigner distribution for each separated signal component is shown in Fig. 3 (d) and (f), for signals  $x_{1i}(t)$  and  $x_{2i}(t)$ , respectively.

**Example 3.** Consider a multivariate three-component signal  $\mathbf{x}(t)$  for  $N = 4$ , for which the  $i$ th channel signal is defined as

$$x_i(t) = x_{1i}(t) + x_{2i}(t) + x_{3i}(t), \quad i = 1, \dots, 4, \quad (23)$$

the components  $x_{1i}(t)$  and  $x_{2i}(t)$  are given by (21) and (22), for  $i = 1, \dots, 4$  whereas the third component has the following form

$$x_{3i}(t) = 0.9e^{-(t/128)^2} e^{-j\pi t/8+j(t/16)^4/100+\varphi_{3i}}, \quad (24)$$

also having the phase  $\varphi_{3i}$ ,  $i = 1, \dots, 4$  simulated as a random number with a uniform distribution drawn from the interval  $[0, 2\pi]$ . The signal from the first channel, its Fourier transform and the multivariate spectrogram are shown in Fig. 4 (a)–(c) respectively.

The Wigner distribution of the analyzed signal is shown in Fig. 5 (a), whose inverse matrix  $\mathbf{R}$  is the subject of eigenvalue decomposition. The obtained eigenvalues are shown in Fig. 5 (b) while Fig. 5 (c), (e) and (g) show the pseudo Wigner distributions of the eigenvectors with largest eigenvalues in subplot (b), and illustrate that the components are not separated. Namely, as in the previous example, the intersected components are not orthogonal and consequently, each considered eigenvector contains a linear combination of signal components. For the obtained eigenvectors, we apply the proposed minimization procedure, in order to find the coefficients that combine these eigenvectors to produce the best concentration, corresponding to the signal components. All three signal components were successfully extracted, as shown in Fig. 5 (d), (f) and (h).

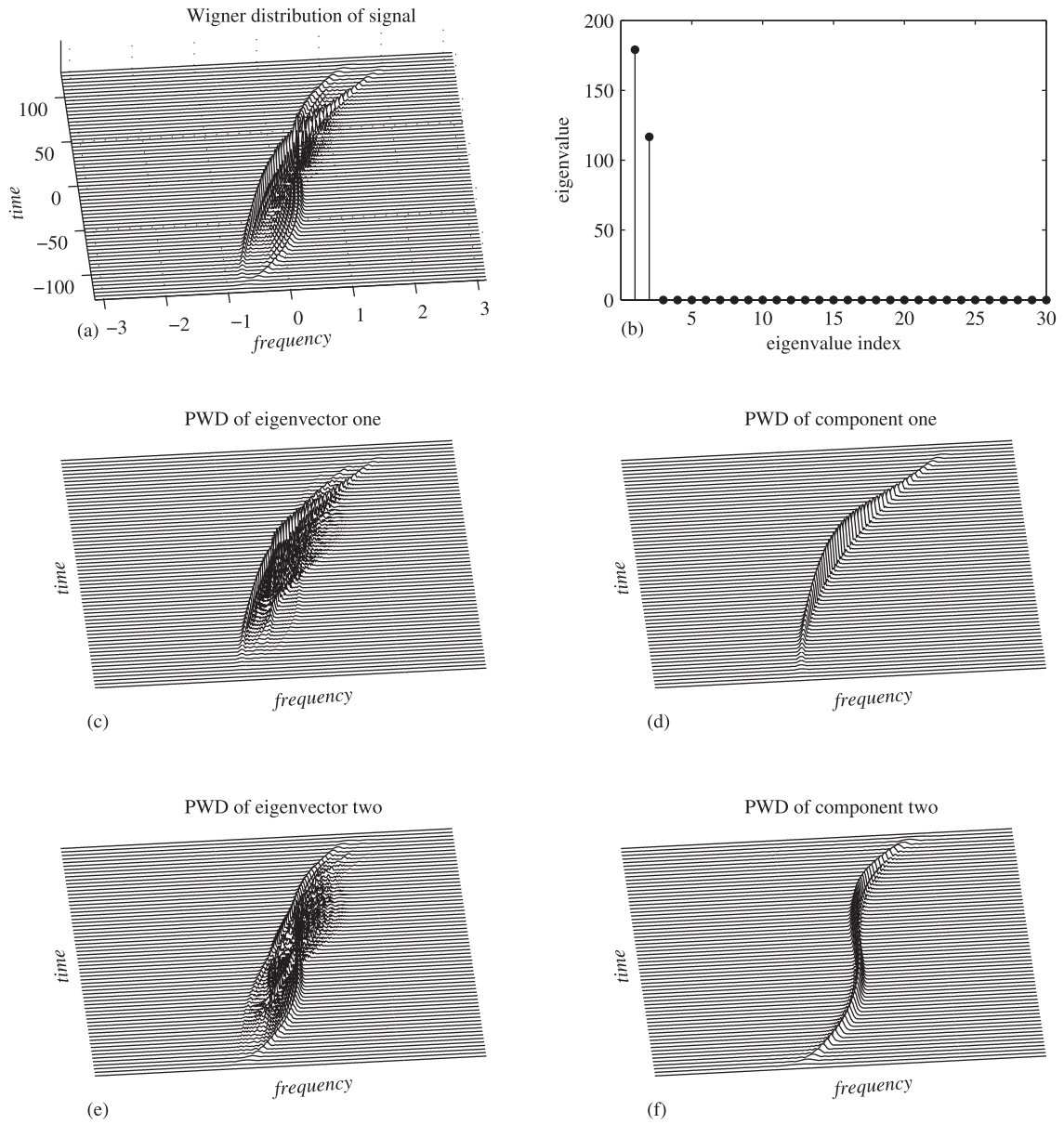


**Fig. 3.** Decomposition of the bivariate two-component signal from Example 2. (a) WD of the analyzed signal. (b) Eigenvalues of the autocorrelation matrix  $\mathbf{R}$ . (c) and (e): PWD of the first and second eigenvector. (d) and (f) PWDs of extracted signal components.

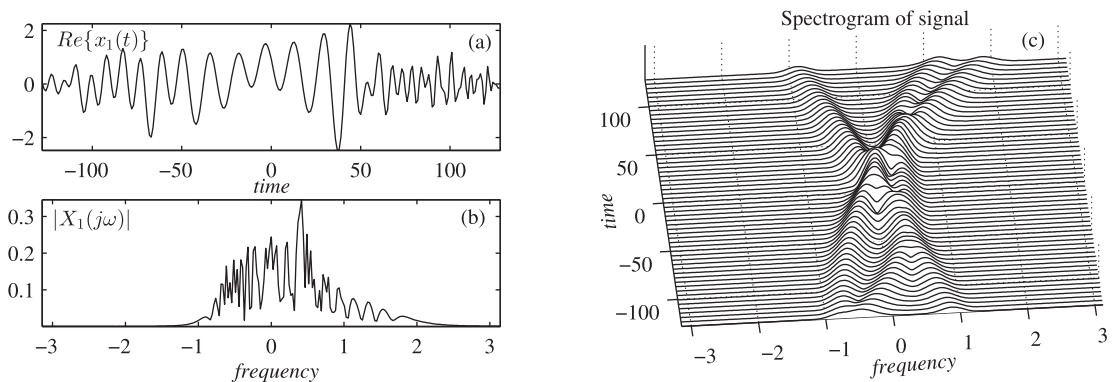


**Fig. 4.** Multi-variate signal having 3 components, with  $N = 4$  shown in: (a) time domain, (b) frequency domain, (c) time-frequency domain (spectrogram).

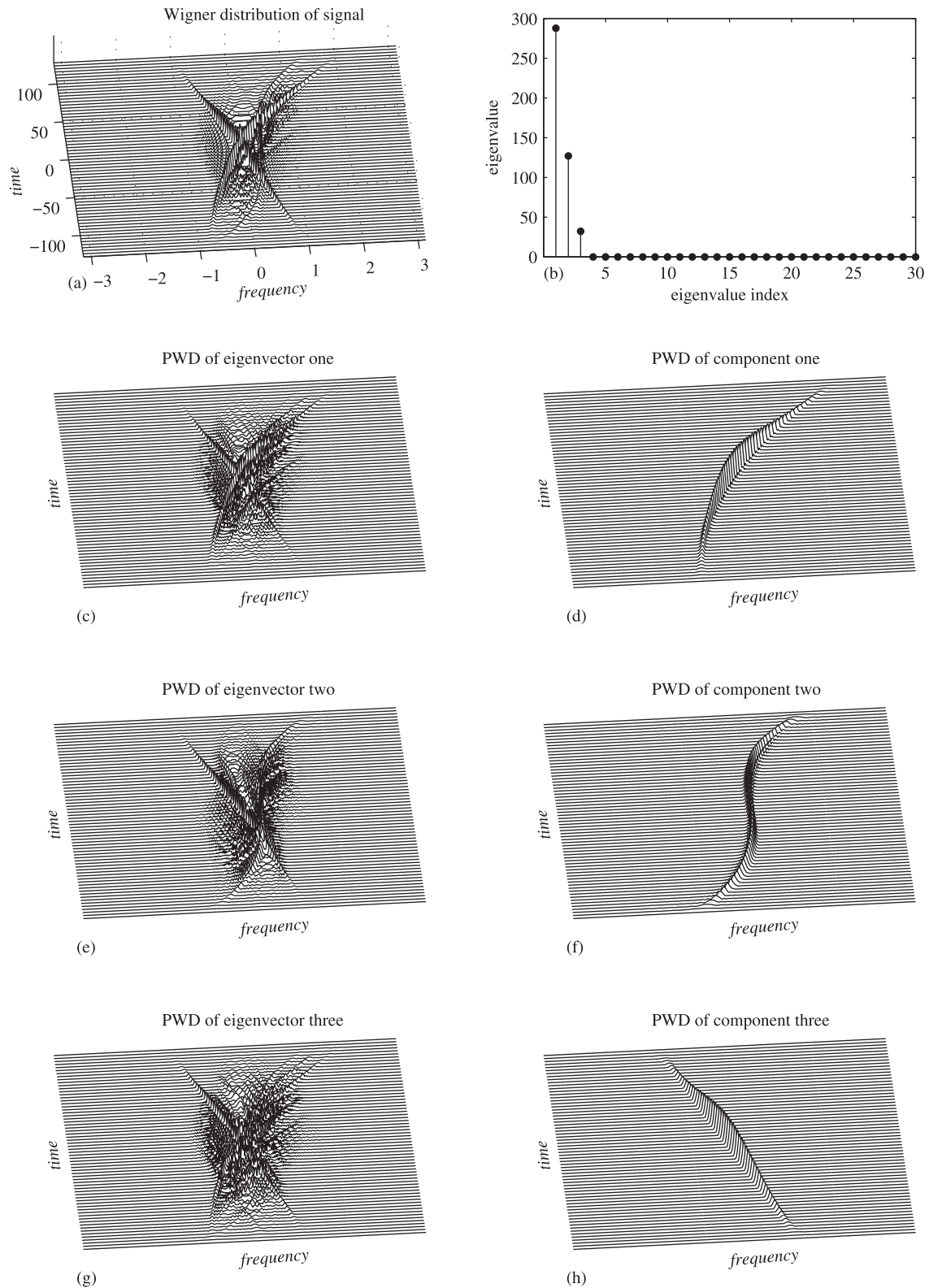


**Fig. 5.** Decomposition of a multivariate signal from Example 3 with  $N = 4$ , having three components (auto-terms). (a) Wigner distribution of the signal. (b) Eigenvalues of the autocorrelation matrix  $\mathbf{R}$ . (c), (e) and (g): PWD of the first, second and third eigenvector; (d), (f) and (h) PWDs of extracted signal components.

**Example 4.** A multivariate signal  $\mathbf{x}(t)$  consisted of three intersected components and two non-overlapping components in the TF plane, given by

$$\mathbf{x}_i(t) = x_{1i}(t) + x_{2i}(t) + x_{3i}(t) + x_{4i}(t) + x_{5i}(t). \quad (25)$$

The signals from each of  $N = 3$  channels are defined as follows

$$x_{1i}(t) = e^{-(t/96)^2} e^{j(-\pi(t/16)^2/5 + \varphi_{1i})} \quad (26)$$

$$x_{2i}(t) = 1.2e^{-(t/96)^2} e^{j(\pi(t/16)^3/32 + 3\pi(t/16)^2/10 + \varphi_{2i})} \quad (27)$$

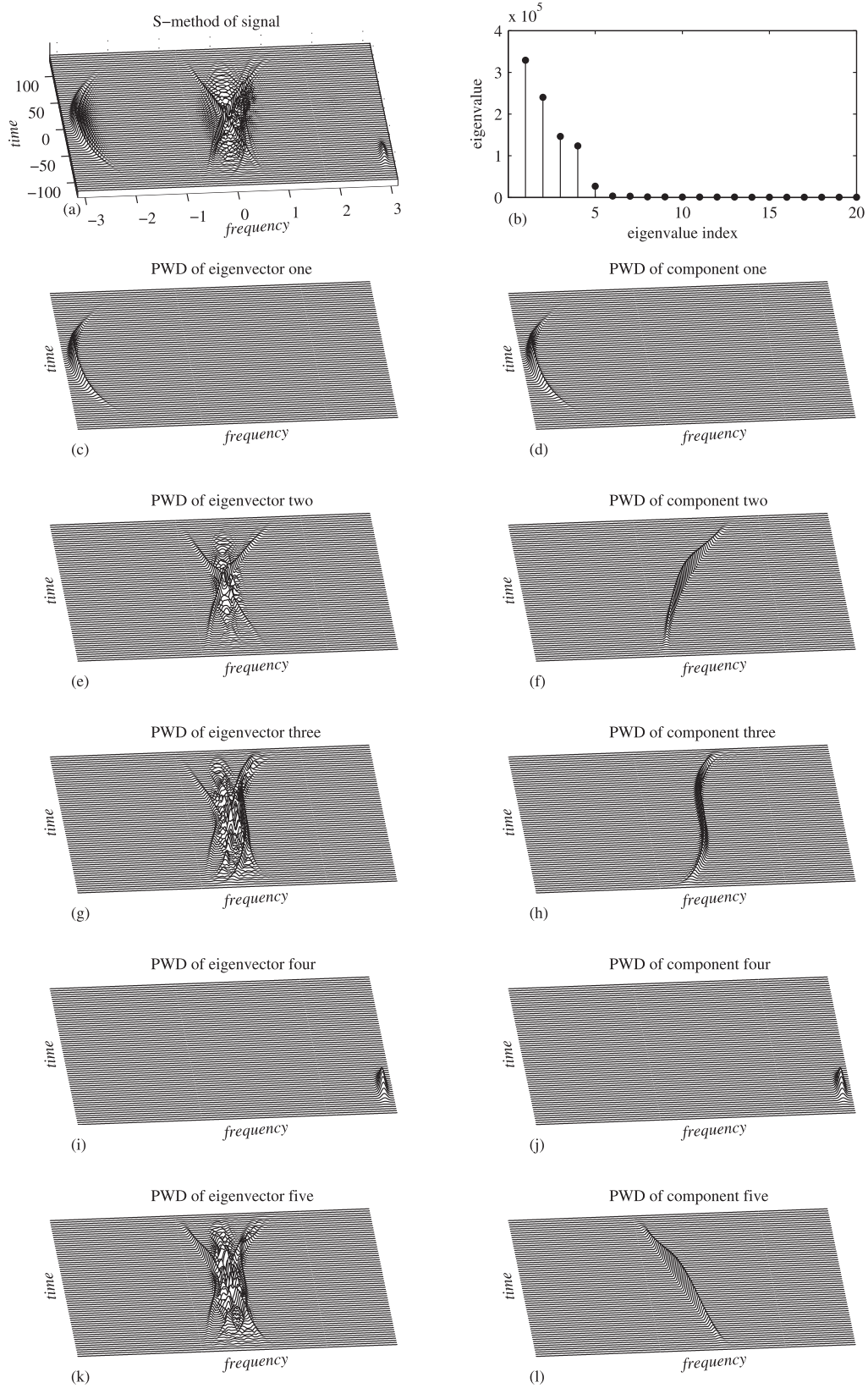


**Fig. 6.** Decomposition of multivariate five-component signal from Example 4 with  $N = 3$ , based on S-method as underlying TFR. (a) S-method of the analyzed signal. (b) eigenvalues of the autocorrelation matrix  $\mathbf{R}$ . (c), (e), (g), (i), (k) PWDs of eigenvectors corresponding to the largest five eigenvalues. (d), (f), (h), (j) and (l) PWDs of extracted signal components.

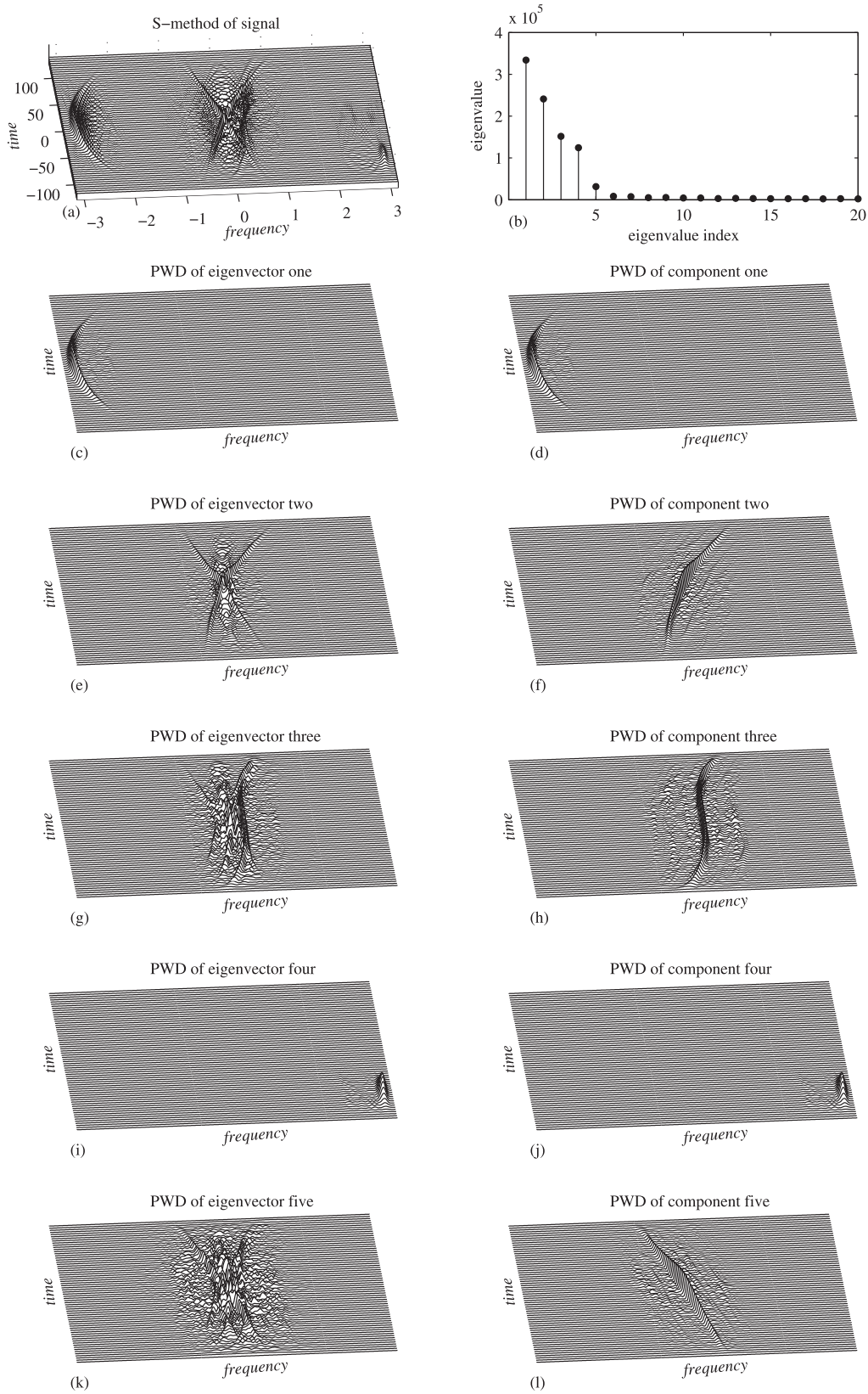


**Fig. 7.** Decomposition of the noisy multivariate five-component signal from Example 4 with  $N = 3$ , based on S-method as underlying TFR. (a) S-method of the analyzed signal. (b) eigenvalues of the autocorrelation matrix  $\mathbf{R}$ . (c), (e), (g), (i), (k) PWDs of eigenvectors corresponding to the largest five eigenvalues. (d), (f), (h), (j) and (l) PWDs of extracted signal components.

$$x_{3i}(t) = 0.9e^{-(t/128)^2} e^{j(\pi(t/16)^4/200 + \pi t/8 + \varphi_{3i})} \quad (28)$$

$$x_{4i}(t) = e^{-(t/16)^2} e^{j(3\pi t/4 + \varphi_{4i})} \quad (29)$$

$$x_{5i}(t) = e^{-(t/96)^2} e^{j(-6\pi(t/16)^2/25 + \pi t/4 + \varphi_{5i})} \quad (30)$$

where  $i = 1, 2, 3$  denotes the channel index. In this example the S-method is used as the initial TFR, as shown in Fig. 6 (a). Application of the S-method is crucial here since we have five components and a trivariate signal only. The S-method would be able to separate (decompose) all non-overlapping components from one realization. Then, the available realizations are used for the overlapped components only. The eigenvalue decomposition of the S-method inverse autocorrelation matrix  $\mathbf{R}$  produced five eigenvectors, corresponding to the five largest eigenvalues shown in Fig. 6 (b).

As the two non-overlapping signal components are mutually orthogonal and with the rest of intersected components, according to the theory presented in [1], there are exactly two eigenvectors corresponding to these two components (one eigenvector for each component). The pseudo Wigner distribution for these two eigenvectors are shown in Fig. 6 (c) and (i). Therefore, these two components are easily extracted, as shown in Fig. 6 (d) and (j). The three remaining components are obtained based on the proper linear combination of the three corresponding eigenvectors using coefficients  $\beta_i$  obtained by the proposed minimization procedure. The pseudo Wigner distributions of these three remaining eigenvectors are shown in Fig. 6 (e), (g) and (k), whereas the separated components obtained based on their proper linear combination are shown in Fig. 6 (f), (h) and (l).

The same experiment was repeated for the noisy signal  $\hat{\mathbf{x}}(t) = \mathbf{x}(t) + \epsilon(t)$ . The signal from each channel corrupted by additive, white zero-mean complex-valued i.i.d. Gaussian noise  $\epsilon_i(t)$  with the variance of real and imaginary parts  $\sigma^2 = 0.15^2$ . The SNR level for one (linear FM) component was 7.13 dB, that is, quite low. The results of the proposed decomposition approach are presented in Fig. 7, illustrating that the proposed algorithm is robust against the additive Gaussian noise influence.

## 7. Conclusion

Decomposition of non-stationary signals overlapping in the time-frequency plane is still an open problem. Exploiting the fact that the Wigner distribution of multivariate signals exhibits significant cross-term change due to their arbitrary phases whereas the auto-terms are added up in phase, we have revisited the time-frequency based signal components decomposition. In this paper, we have shown that even with a small number of signal channels, relative to the number of components, an accurate decomposition can be performed with an appropriate linear combination of the signal autocorrelation matrix eigenvectors. Next, the decomposition and eigenvector combination algorithms have been proposed. Their efficiency has been illustrated over several examples, which conclusively validate the capability of the proposed algorithm to perform a complete and accurate extraction of overlapped and non-overlapped components. The robustness of the proposed approach has been illustrated over an example on a noisy signal.

## References

- [1] L. Stanković, T. Thayaparan, M. Daković, Signal decomposition by using the S-method with application to the analysis of HF radar signals in sea-clutter, *IEEE Trans. Signal Process.* 54 (11) (2006) 4332–4342.
- [2] Y. Wei, S. Tan, Signal decomposition by the S-method with general window functions, *Signal Process.* 92 (1) (2012) 288–293.
- [3] Y. Yang, X. Dong, Z. Peng, W. Zhang, G. Meng, Component extraction for non-stationary multi-component signal using parameterized de-chirping and band-pass filter, *IEEE SP Lett.* 22 (9) (2015) 1373–1377.
- [4] Y. Wang, Y. Jiang, ISAR imaging of maneuvering target based on the l-class of fourth-order complex-lag PVWD, in: *IEEE Transactions on Geoscience and Remote Sensing*, 48, 2010, pp. 1518–1527.
- [5] I. Orović, S. Stanković, A. Draganić, Time-frequency analysis and singular value decomposition applied to the highly multicomponent musical signals, *Acta Acustica United With Acustica* 100 (2014) 1.
- [6] L. Stanković, M. Daković, T. Thayaparan, *Time-Frequency Signal Analysis with Applications*, Artech House, 2013.
- [7] V. Katkovnik, L. Stanković, Instantaneous frequency estimation using the Wigner distribution with varying and data driven window length, *IEEE Trans. Signal Process.* 46 (9) (1998) 2315–2325.
- [8] V.N. Ivanović, M. Daković, L. Stanković, Performance of quadratic time-frequency distributions as instantaneous frequency estimators, *IEEE Trans. Signal Process.* 51 (1) (2003) 77–89.
- [9] A. Ahrabian, D. Looney, L. Stanković, D. Mandić, Synchrosqueezing-based time-frequency analysis of multivariate data, *Signal Process.* 106 (2015) 331–341.
- [10] J.M. Lilly, S.C. Olhede, Analysis of modulated multivariate oscillations, *IEEE Trans. Signal Process.* 60 (2) (2012) 600–612.
- [11] A. Omidvarnia, B. Boashash, G. Azemi, P. Colditz, S. Vanhatalo, Generalised phase synchrony within multivariate signals: an emerging concept in time-frequency analysis, in: *IEEE International Conference on Acoustics, Speech and Signal Processing (ICASSP)*, Kyoto, 2012, pp. 3417–3420.
- [12] J.M. Lilly, S.C. Olhede, Bivariate instantaneous frequency and bandwidth, *IEEE Trans. Signal Process.* 58 (2) (2010) 591–603.
- [13] B. Boashash, Estimating and interpreting the instantaneous frequency of a signal. I. fundamentals, *Proc. IEEE* 80 (4) (1992) 520–538, doi:10.1109/5.135376.
- [14] J.C. Wood, D.T. Barry, Radon transformation of time-frequency distributions for analysis of multicomponent signals, *IEEE Trans. Signal Process.* 42 (11) (1994) 3166–3177.
- [15] G. Lopez-Risueno, J. Grajal, O. Yeste-Ojeda, Atomic decomposition-based radar complex signal interception, *IEE Proc. Radar, Sonar Navig.* 150 (4) (2003) 323–331.
- [16] L. Stanković, M. Daković, T. Thayaparan, V. Popović-Bugarin, Inverse radon transform based micro-Doppler analysis from a reduced set of observations, *IEEE Trans. AES* 51 (2) (2015) 1155–1169.
- [17] M. Daković, L. Stanković, Estimation of sinusoidally modulated signal parameters based on the inverse radon transform, in: *ISPA 2013, Trieste, Italy, 2013*, pp. 302–307.
- [18] D.P. Mandić, N.u. Rehman, Z. Wu, N.E. Huang, Empirical mode decomposition-based time-frequency analysis of multivariate signals: the power of adaptive data analysis, *IEEE Signal Process. Mag.* 30 (2013) 74–86.
- [19] S.M.U. Abdullah, N.u. Rehman, M.M. Khan, D.P. Mandić, A multivariate empirical mode decomposition based approach to pansharpening, *IEEE Trans. Geosci. Remote Sens.* 53 (7) (2015) 3974–3984.
- [20] A. Hemakom, A. Ahrabian, D. Looney, N.u. Rehman, D.P. Mandić, Nonuniformly sampled trivariate empirical mode decomposition, in: *IEEE International Conference on Acoustics, Speech and Signal Processing (ICASSP 2015)*, South Brisbane, QLD, 2015, pp. 3691–3695.
- [21] G. Wang, C. Teng, K. Li, Z. Zhang, X. Yan, The removal of EOG artifacts from EEG signals using independent component analysis and multivariate empirical mode decomposition, *IEEE J. Biomed. Health Inf.* 20 (5) (2016) 1301–1308.
- [22] S. Tavildar, A. Ashrafi, Application of multivariate empirical mode decomposition and canonical correlation analysis for EEG motion artifact removal, in: *2016 Conference on Advances in Signal Processing (CASP)*, Pune, 2016, pp. 150–154.
- [23] Y. Zhang, M.G. Amin, B.A. Obeidat, Polarimetric array processing for nonstationary signals, in: *Adaptive Antenna Arrays: Trends and Applications*, Springer, 2004, pp. 205–218.
- [24] L. Stanković, A measure of some time-frequency distributions concentration, *Signal Process.* 81 (2001) 621–631.
- [25] J.C. Spall, *Introduction to Stochastic Search and Optimization*, Wiley, ISBN 0-471-33052-3.
- [26] J. Larson, S.M. Wild, A batch, derivative-free algorithm for finding multiple local minima, *Optim. Eng.* 17 (1) (2016) 205228, doi:10.1007/s11081-015-9289-7.
- [27] A. Neumaier, Complete search in continuous global optimization and constraint satisfaction, *Acta Numerica* 13 (1) (2004).
- [28] W. Hu, K. Wu, P.P. Shum, N.I. Zheludev, C. Soci, All-optical implementation of the ant colony optimization algorithm, *Sci. Rep.* 6 (2016), doi:10.1038/srep26283.
- [29] S. Kirkpatrick, C.D. Gelatt, M.P. Vecchi, Optimization by simulated annealing, *Science* 220 (4598) (1983) 671–680, doi:10.1126/science.220.4598.671.
- [30] R. Chelouaha, P. Siarry, Genetic and neldermead algorithms hybridized for a more accurate global optimization of continuous multimimima functions, *Eur. J. Oper. Res.* 148 (2) (2003) 335348.
- [31] A. Cichocki, S. Amari, *Adaptive Blind Signal and Image Processing: Learning Algorithms and Applications*, 1, John Wiley and Sons, 2002, pp. 191–193.